Published online 6 December 2016

Nucleic Acids Research, 2017, Vol. 45, No. 6 ***e45***
doi: 10.1093/nar/gkw1205

A specific DNA-nanoprobe for tracking the activities of human apurinic/apyrimidinic endonuclease 1 in living cells

Junqiu Zhai, Yibin Liu, Shan Huang, Simin Fang and Meiping Zhao*

Beijing National Laboratory for Molecular Sciences and MOE Key Laboratory of Bioorganic Chemistry and Molecular Engineering, College of Chemistry and Molecular Engineering, Peking University, Beijing 100871, China

Received September 02, 2016; Revised October 16, 2016; Editorial Decision November 17, 2016; Accepted November 19, 2016

ABSTRACT

Human apurinic/apyrimidinic endonuclease/redox effector factor 1 (APE1) is an essential DNA repair protein. Herein, we demonstrate that avidin-oriented abasic site-containing DNA strands (AP-DNA) on the surface of silica coated magnetic nanoparticles (SiMNP) can selectively respond to APE1 while resist the digestion by other nucleases. Mechanism studies have revealed that avidin may serve as an organizer protein and recruit APE1 to the DNA substrates on the nanoparticles via strong and specific interactions. Taking advantage of this newly disclosed property, we for the first time successfully displayed the intracellular activities of APE1 in living cells by fluorescence imaging. The avidin organized AP-DNA-SiMNP assembly holds great potential for enzyme-mediated release of drugs inside tumor cells which often contain higher levels of APE1 than normal cells.

INTRODUCTION

Apurinic/apyrimidinic endonuclease/redox effector factor 1 (APE1) plays key roles in the base excision repair (BER) pathway of DNA lesions to maintain the genome stability (1–5). It is also involved in regulating cellular responses to oxidative stress conditions. Abnormal expression/localization of APE1 has been found in tumor cells (6–8). Up to now, a number of approaches have been developed for the detection of APE1, such as enzyme-linked immunosorbent assay (9), electrochemical immunoassay (10), electrochemiluminescence immunosensor (11) and fluorescent DNA probes (12,13). However, most of them are only suitable for *in-vitro* applications. It remains a difficult issue to visualize the activity of this important protein within living cells due to the lack of specific tools. Silica nanoparticles (SiNPs) or silica coated magnetic core–shell NPs (SiMNPs) have been widely used to deliver DNA molecules into various types of cells for intracellular diagnosis or genetic therapy (14–19). The methods are straightforward, low-cost and biocompatictble. Several studies have shown that the SiMNPs can protect the immobilized DNA from nuclease digestion (20–22). But the mechanisms for such protection effects are still uncertain.

Herein, we demonstrate that biotin-labeled abasic site-containing dsDNA (AP-DNA) attached to the avidin-modified surface of SiMNPs can be specifically and efficiently cleaved by APE1 while resistant to the nonspecific digestion by other nucleases. This unique property offers the possibility of APE1-mediated cleavage of DNA sequence at predetermined site in the intracellular environment which are admired in intracellular imaging and cancer therapy since APE1 levels often increase in cancer cells (7). In this work, we systematically investigated the mechanisms for the avidin-organized molecular assembly. Moreover, we successfully visualized the intracellular activities of APE1 in living cells by fluorescence imaging and observed the variation of the enzyme activity under different conditions.

MATERIALS AND METHODS

Chemical reagents and materials

The DNA oligonucleotides were synthesized and purified by HPLC (Sangon Biotech Co., China). The sequences of all the DNA strands that have been studied in this work are summarized in Supplementary Table S1. Silica-coated magnetic Fe_3O_4 nanoparticles (SiMNPs) were purchased from Suzhou Nord Derivatives Pharm-Tech Co. Ltd. (Suzhou, China). Avidin, streptavidin, 1-ethyl-3-(3-dimethylaminopropyl) carbodiimide hydrochloride (EDC), *N*-hydroxysulfosuccinimide sodium salt (sulfo-NHS) and 7-nitroindole-2-carboxylic acid were purchased from Sigma Chemical Co. (St. Louis. MO, USA). Apurinic/apyrimidinic endonuclease I (APE1), uracil–DNA glycocasylase (UDG), deoxyribonuclease I (DNase I), exonuclease III (Exo III), exonuclease I (Exo I), lambda exonuclease (λ exo), T5 exonuclease (T5 Exo), T7 exonu-

*To whom correspondence should be addressed. Tel: +86 10 62758153; Fax: +86 10 62751708; Email: mpzhao@pku.edu.cn
Present address: Meiping Zhao, College of Chemistry and Molecular Engineering, Peking University, Beijing 100871, China.

clease (T7 Exo) and their corresponding buffers (Supplementary Table S2) were all purchased from New England Biolabs (NEB, USA). Hoechst 33342, propidium iodide (PI) and cell-counting kit (CCK-8) were all obtained from Dojindo Laboratories (Kumamoto, Japan). *tert*-Butyl hydroperoxide (TBHP) were purchased from Aladdin Industrial Inc. Dulbecco's modified Eagle's medium (DMEM) and Dulbecco's phosphate buffer solution without calcium and magnesium (DPBS) were purchased from Corning (Manassas, VA, USA). Human cervical carcinoma cell line (HeLa) was purchased from ATCC (Manassas, VA, USA).

Synthesis of DNA-nanoprobes

Nanoprobe A. To 2.0 ml of 0.5 mg/ml of carboxyl-functionalized Fe_3O_4@SiO_2 NPs (SiMNPs) in ddH_2O, 4.0 mg of EDC and 10.0 mg of Sulfo-NHS were added and mixed well. The solution was incubated at room temperature with gentle shaking for 30 min. Then, 100 μl of 2.0 mg/ml avidin was added and the obtained solution was incubated at room temperature with gentle shaking for 8 h. After magnetic separation and washing for three times, the avidin modified nanoparticles (SiMNP@AVD) were dispersed in 2.0 ml of ddH_2O, to which the pre-annealed 46-Biotin/18-FAM DNA duplex (Supplementary Table S1) was added at a final concentration of 1.0 μM. After incubation for 1 h, the resultant solution was magnetically separated and washed for three times with 0.1 M phosphate-buffered saline (pH 7.4, PBS) to remove the unreacted DNA. The obtained Nanoprobe A-U (Fe_3O_4@SiO_2@AVD-dsDNA) was resuspended in 2.0 ml 0.1 M PBS for further use or stored at 4°C.

To prepare Nanoprobe A, 5.0 μl of 1.0 mg/ml Nanoprobe A-U and 5.0 μl of 10× buffer 1.1 were first mixed well in a 50 μl PCR tube containing 37 μl of distilled water. Then, 1.0 μl of 500 U/ml UDG was added to the mixture solution to remove the uracil in Nanoprobe A-U. After 2 min, the obtained Nanoprobe A (Fe_3O_4@SiO_2@AVD-AP-DNA) was immediately used for further analysis.

Nanoprobe S. The synthetic procedures for Nanoprobe S are generally the same as those for Nanoprobe A except that avidin has been replaced by streptavidin. In brief, 4.0 mg EDC, 10.0 mg Sulfo-NHS and 1.0 mg of carboxyl-functionalized Fe_3O_4@SiO_2 NPs were mixed well in 2.0 ml of pure water. After 30-min incubation at room temperature with gentle shaking, 100 μl of 2.0 mg/ml streptavidin was added and the solution was incubated for 8 h at room temperature with gentle shaking. After magnetic separation and washing for three times, the strepavidin modified nanoparticles (SiMNP@SA) were dispersed in 2.0 ml of ddH_2O, to which the pre-annealed 46-Biotin/18-FAM DNA duplex was added at a final concentration of 1.0 μM. After incubation for 1 h, the resultant solution was magnetically separated and washed for three times with 0.1 M phosphate-buffered saline (pH 7.4, PBS) to remove the unreacted DNA. The obtained Nanoprobe S-U (Fe_3O_4@SiO_2@SA-dsDNA) was resuspended in 2.0 ml 0.1 M PBS for further use or stored at 4°C.

To prepare Nanoprobe S, 5.0 μl of 1.0 mg/ml Nanoprobe S-U and 5.0 μl of 10× buffer 1.1 were first mixed well in a 50 μl PCR tube containing 37 μl of distilled water. Then 1.0 μl of 500 U/ml UDG was added to the mixture solution to remove the uracil in Nanoprobe S-U. After 2 min, the obtained Nanoprobe A (Fe_3O_4@SiO_2@SA-AP-DNA) was immediately used for further analysis.

Nanoprobe C. 4.0 mg EDC, 10.0 mg Sulfo-NHS and 1.0 mg of carboxyl-functionalized Fe_3O_4@SiO_2 NPs were mixed well in 2.0 ml of pure water. After 30-min incubation at room temperature with gentle shaking, the pre-annealed 46-NH_2/18-FAM DNA duplex was added at a final concentration of 1.0 μM. After incubation for 8 h at room temperature with gentle shaking, the resultant solution was magnetically separated and washed for three times with 0.1 M phosphate-buffered saline (pH 7.4, PBS) to remove the unreacted DNA. The obtained Nanoprobe C-U (Fe_3O_4@SiO_2@CO-NH_2-dsDNA) was resuspended in 2.0 ml 0.1 M PBS for further use or stored at 4°C.

To prepare Nanoprobe C, 5.0 μl of 1.0 mg/ml Nanoprobe C-U and 5.0 μl of 10× buffer 1.1 were first mixed well in a 50 μl PCR tube containing 37 μl of distilled water. Then 1.0 μl of 500 U/ml UDG was added to the mixture solution to remove the uracil in Nanoprobe C-U. After 2 min, the obtained Nanoprobe C (Fe_3O_4@SiO_2@ CO-NH_2-AP-DNA) was immediately used for further analysis.

Nanoprobe N. 4.0 mg EDC, 10.0 mg Sulfo-NHS and 2.0 nmol pre-annealed HOOC-46/FAM-18 DNA duplex were mixed well in 1.0 ml of pure water. After 30-min incubation at room temperature with gentle shaking, the resultant solution was added to 1.0 ml of 1.0 mg/ml of amino-functionalized Fe_3O_4@SiO_2 NPs. After incubation for 8 h at room temperature with gentle shaking, the resultant solution was magnetically separated and washed for three times with 0.1 M phosphate-buffered saline (pH 7.4, PBS) to remove the unreacted DNA. The obtained Nanoprobe N-U (Fe_3O_4@SiO_2@ NH_2-CO-dsDNA) was resuspended in 2.0 ml 0.1 M PBS for further use or stored at 4°C.

To prepare Nanoprobe N, 5.0 μl of 1.0 mg/ml Nanoprobe–N-U and 5.0 μl of 10× buffer 1.1 were first mixed well in a 50 μl PCR tube containing 37 μl of distilled water. Then 1.0 μl of 500 U/ml UDG was added to the mixture solution to remove the uracil in Nanoprobe N-U. After 2 min, the obtained Nanoprobe N (Fe_3O_4@SiO_2@ NH_2-CO-AP-DNA) was immediately used for further analysis.

In-vitro enzymatic reactions

All the *in-vitro* enzymatic reactions were carried out in 50 μl sealed PCR tubes. The fluorescence intensity of the reaction solution was monitored in real time on Rotor-Gene Q (Qiagen, Germany). The thermal program was 250 cycles at 37°C with 5 s per cycle, and the fluorescence was measured at the end of each cycle. The excitation and emission wavelengths are 470 and 510 nm, respectively. The fluorescence gain level is 10. The reaction buffers for different enzymes are listed in Supplementary Table S2. The concentration of the nanoprobes used for the enzymatic reactions was fixed at 0.1 mg/ml unless otherwise stated.

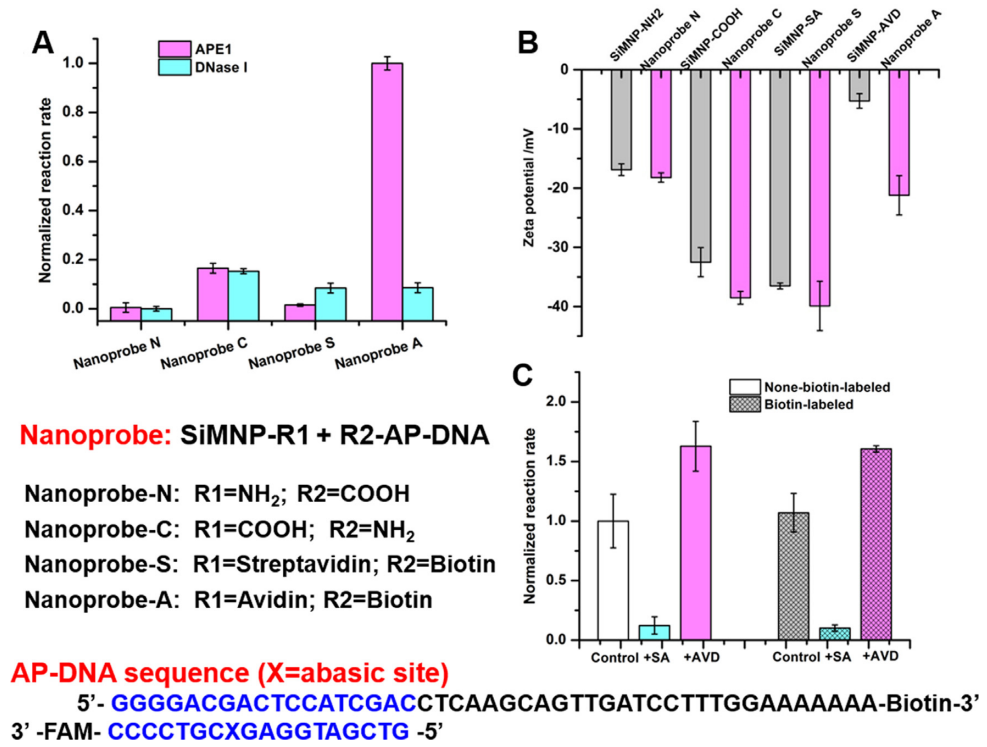

Figure 1. (**A**) Comparison of the responses of four different Nanoprobes to APE1 and DNase I. (**B**) Zeta potential values of the four different Nanoprobes. (**C**) Influences of free avidin or streptavidin molecules on the reactions between APE1 and AP-DNA in homogeneous solutions. Probe 1 (BHQ1-46-biotin/18-FAM duplex, Supplementary Table S1) and Probe 1' (BHQ1-46/18-FAM duplex) were used as the Biotin-labeled and Non-biotin-labeled AP-DNA, respectively. All experiments were repeated at least three times.

RESULTS AND DISCUSSION

We investigated four different approaches to attach AP-DNA (Supplementary Table S1) to the surface of Fe_3O_4@SiO_2 NPs and compared the digestion rates of the immobilized AP-DNA in the presence of APE1 and DNase I, respectively (Figure 1A). Since magnetic nanoparticles had very strong quenching effect on the fluorescence of FAM and other dyes (23,24), no additional quencher was attached to the AP-DNA. Nanoprobe N was prepared by directly conjugating carboxyl-labeled AP-DNA to amino-modified SiMNPs, which showed no responses to either APE1 or DNase I, indicating complete inhibition of the interactions between the DNA and nucleases by the SiMNPs. These results were consistent with the previous findings (20–22). In contrast, when amino-labeled AP-DNA was directly conjugated to carboxyl-modified SiMNPs, the obtained Nanoprobe C showed observable cleavage signals for both APE1 and DNase I. Then we first coated the surface of SiMNPs with streptavidin or avidin, then attached the biotinlyted DNA sequences to the streptavidin or avidin modified surfaces (25). Surprisingly, the streptavidin-conjugated DNA probe (Nanoprobe S) showed weaker responses to both nucleases than Nanoprobe C, though they have almost similar zeta potential values (Figure 1B). By contrast, the avidin-conjugated DNA probe (Nanoprobe A) showed significantly higher fluorescence signals to APE1 than other three nanoprobes, while its response to DNase I was as low as that of Nanoprobe S (Figure 1A).

Above results indicated that the conjugation chemistry of DNA molecules on the surface of SiMNPs had significant effects on the interactions between the attached DNA and nucleases. Nanoprobe C and Nanoprobe S have much more negative charges than Nanoprobe N, which may orient the immobilized DNA molecules to a more extended conformation on the surface of SiMNPs. Thus their digestion rates by DNase I were relatively higher than that of Nanoprobe N. However, the zeta potential data could not explain the distinct interactions between Nanoprobe A and APE1. APE1 (pI = 8.33) and avidin (pI = 10.0) both have positive charges in the reaction buffer (pH 7.0, Supplementary Table S2), while DNase I (pI = 4.7) bears more negative charges. These electrostatic interaction features were not the major reasons for the results in Figure 1A.

By comparison of the results of Nanoprobe S with those of Nanoprobe C, the density of DNA may not be a major factor that dominate the digestion reactions. Moreover, since APE1 is also highly dependent on the presence of Mg^{2+} (26), the previously suggested mechanisms of low metal ion concentration for the inhibited digestion of the plasmid DNA by DNase I (20,21) seemed to be not supported by above results. Wang *et al.* proposed that the conformational change of DNA after binding to the surface of the NPs will protect DNA from cleavage (20). From the results shown in Figure 1, these conformational changes had little effects on the digestion of DNA by APE1, thus the contribution of this factor was also very limited.

To find out the real reasons for our experimental results, we investigated the influences of free avidin molecules on the reactions between APE1 and AP-DNA in homogeneous solutions. Probe 1 (BHQ1-46-biotin/18-FAM duplex) has the same sequence as the AP-DNA immobilized on Nanoprobe A. BHQ1 was labeled to the 5′ end of Probe 1 so that the fluorescence of FAM can be efficiently quenched in the absence of target APE1. Probe 1' (BHQ1-46/18-FAM duplex) is a control probe for Probe 1 which was not labeled with biotin at the 3' end. From Figure 1C, addition of avidin to the reaction solution notably enhanced the digestion rate of both biotin-labeled (Probe 1) and non-biotin-labled (Probe 1') AP-DNA by APE1, indicating that avidin itself has a tendency to interact with APE1 which is independent on biotin. By contrast, the enzymatic reactions of DNase I and Exo III were notably inhibited in the presence of avidin (Supplementary Figures S1 and S2). The influences of streptavidin on the enzymatic reactions of the three nucleases were also tested, which were found to be quite different from those of avidin (Figure 1C, Supplementary Figures S1 and S2). These results substantially indicated that additional proteins can have significant influences on the DNA-enzyme interactions.

To further clarify the specific interactions between avidin and APE1, we performed a surface plasmon resonance (SPR) measurement by immobilization of APE1 on the chip surface and injection of avidin as an analyte. Streptavidin was also tested in the same manner for comparison. As shown in Figure 2A, avidin showed significant binding with APE1 ($K_D = 3.2$ nM), while streptavidin only showed very weak interactions with APE1 (Supplementary Figure S3). Then we further incubated APE1 solution with the avidin-modified SiMNPs. For comparison, RNase A (pI = 9.6) which also has positive charges as APE1 and Exo III (Mr = 31 kDa) which has similar size as APE1 (Mr = 33 kDa) were also tested. Figure 2B showed that APE1 was selectively retained by the avidin-SiMNPs, while other two nucleases showed negligible interactions with either the SiMNPs or the avidin modified SiMNPs.

Above results clearly indicated that the interactions between avidin and APE1 were strong enough to recruit the APE1 in the solution to the surface of SiMNPs. A possible model was proposed for the specific interactions between avidin, APE1 and the DNA probe (Scheme 1). The specificity might be attributed to the interrelated interactions among surface proteins on SiMNPs, enzymes and DNA substrates, which significantly facilitated the binding and cleavage of DNA by APE1. Taken the data in Figure 1C and 2B together, avidin could not only recruit APE1 to the surface of SiMNPs, but also notably enhance the activity of APE1 in the digestion of the AP site. This is most likely because the binding of APE1 to avidin induces the conformation change of APE1, which is more close to the active state of the enzyme, thus greatly accelerated the subsequent incision reactions. More detailed mechanisms merit further investigation.

Figure 3A and B shows that Nanoprobe A can rapidly respond to APE1 at different concentrations with a linear range from 0.01 to 1.0 U/ml and a detection limit of 0.01 U/ml. This is more sensitive than the previously developed DNA fluorescent probe for *in-vitro* APE1 detection (13). Figure 3C summarizes the selectivity of Nanoprobe A for APE1 against other possibly coexisting nucleases. The fluorescence signal of DNase I at the tested concentration as high as 5.0 U/ml was <10% of that of APE1 at 2.0 U/ml, indicating excellent selectivity of Nanoprobe A in the detection of APE1 against DNase I. Exonuclease III (Exo III) is both a 3′−5′ exonuclease and an AP endonuclease, thus it may also cleave the AP site and generate fluorescence signals. Figure 3C shows that the fluorescence signal of 4.0 U/ml of Exo III was comparable to ∼20% of 2.0 U/ml of APE1, indicating that Nanoprobe A was much more sensitive to APE1 than to Exo III. The influences of other exonucleases on the detection of APE1 were negligible.

The transmission electron microscopic (TEM) images and dynamic light scattering (DLS) measurement results showed that Nanoprobe A has a regular spherical morphology with an average hydration diameter of about 67 nm (Supplementary Figure S4, Supplementary Table S3). The amount of DNA attached to the SiMNPs was estimated by measurement of the DNA concentration in the supernatant before and after the immobilization reaction. For Nanoprobe A, the number of DNA duplexes conjugated to each nanoparticle was calculated to be 98 ± 8. The efficiency of UDG in removal of the uracil in the DNA duplexes attached to the nanoparticles were examined by changing the UDG concentration and treatment time. From the results shown in Supplementary Figure S5, increase of the UDG concentration did not help to improve the yield of AP-sites; whereas prolongation of the treatment time may lead to complete removal of the uracil in Nanoprobe A-U. Since about 80% of the uracils had been removed in the first 2 min and the amount of the AP-DNA duplexes were high enough for the subsequent reaction with APE1, we adopted the treatment conditions of 10 U/ml of UDG for 2 min. Under this condition, the obtained Nanoprobe A could be effectively used to measure the activity of APE1.

For 0.1 mg/ml Nanoprobe A, it was observed that 1.0 M NaOH can completely destroy the AP sites. Employing NaOH-treated Nanoprobe A as the positive control, we also evaluated the digestion efficiency of APE1 on Nanoprobe A. As shown in Supplementary Figure S6, the cleavage rate of Nanoprobe A by 1.0 U/ml of APE1 was close to that of 1.0 M NaOH. After about 10 min, all the AP sites on Nanoprobe A had been cleaved by both APE1 and NaOH, which substantially proved the high digestion efficiency of APE1 on Nanoprobe A. The digestion rates of APE1 on Nanoprobe A were also compared with those on the naked DNA substrates. For 0.1 mg/ml of Nanoprobe A which contained about 94 ± 8 nM of ds DNA in the 50 μl reaction solution, the digestion rate by 1.0 U/ml of APE1 was observed to be 0.21 ± 0.01 a.u./s. Then we measured the digestion rate of 100 nM free Probe 1′ by 1.0 U/ml of APE1, which was found to be 0.18 ± 0.02 a.u./s under the same conditions. The slightly higher reaction rate of Nanoprobe A may be attributed to the presence of avidin on the surface of the nanoparticles, which may help recruit APE1 to the AP-DNA substrates and enhance the digestion activity of APE1 on the AP sites. The cytotoxicity of Nanoprobe A was also examined by using the Cell Counting Kit-8 (CCK-8) and proved to be very low (Supplementary Figure S7).

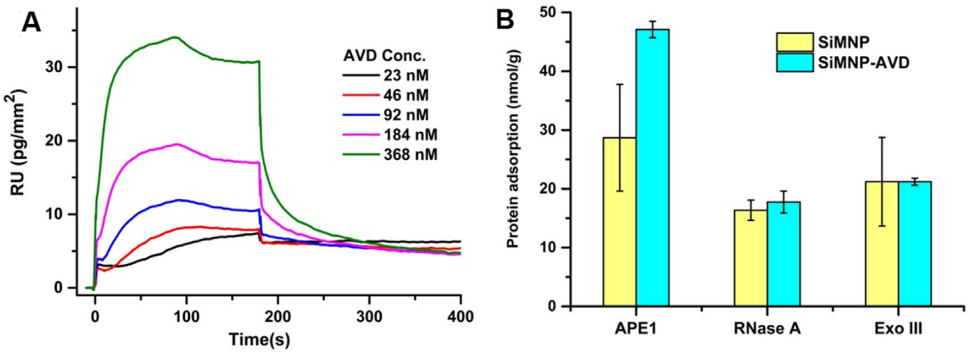

Figure 2. (**A**) SPR measurement results of the interactions between immobilized APE1 and avidin. (**B**) Selective binding of APE1 by immobilized avidin. For comparison, RNase A which has the same pI as APE1 and Exo III which has the same molecular weight as APE1 were also tested. All experiments were repeated at least three times.

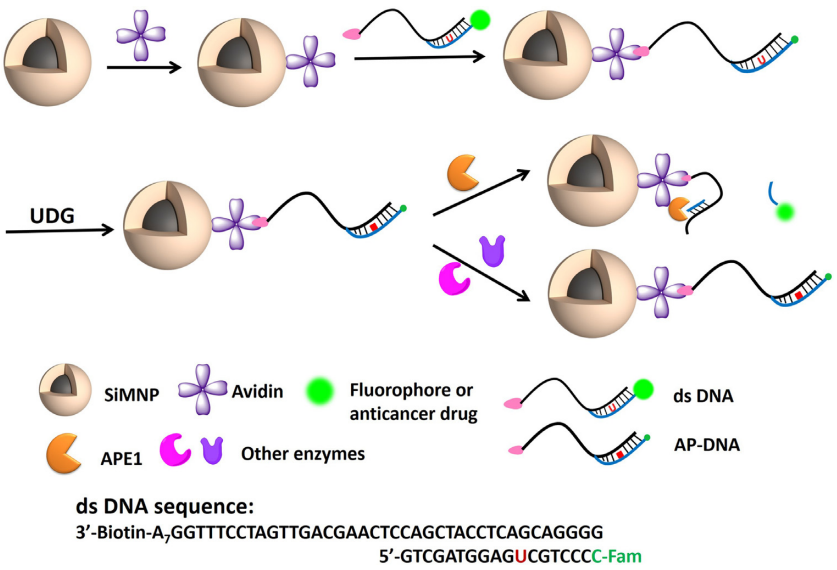

Scheme 1. Schematic representation of a possible model for the specific interactions between the avidin-modified SiMNPs and APE1 which determines the selectivity of Nanoprobe A toward APE1. The avidin organized AP-DNA-SiMNP assembly enables cleavage of Nanoprobe A at predetermined specific site in the intracellular environment. Nanoprobe A-U was first prepared, then the nanoparticles were treated with UDG to obtain Nanoprobe A.

Next, we attempted to deliver Nanoprobe A into living cells to monitor the activity of APE1 in situ. Hoechst 33342 (a blue fluorescent dye) and Lyso-Tracker Red (a red fluorescent dye) were used to stain the nucleus and lysosome of the living cells, respectively. As shown in Figure 4, the fluorescence signals of Nanoprobe A could be clearly observed in the cytoplasm after 45 min and the intensity gradually increased to the maximum at 120 min.

To confirm that the intracellular fluorescence signals were generated from the cleavage of AP-site of Nanoprobe A by APE1, Nanoprobe A-U which has the same sequence as Nanoprobe A except that the uracil was not removed by UDG treatment (see Supplementary Table S1) was used as a control probe and transferred into cells to monitor the background signals originated from other sources inside the cells. From Figure 5, little fluorescence of Nanoprobe A-U could be observed even after incubation for 120 min, which substantially proved the specificity of Nanoprobe A. We also monitored the variation of APE1 activity in living cells after treatment with different drugs. Tert-butyl hydroperoxide (TBHP) (27) and 7-nitroindole-2-carboxylicacid (NCA) (28) were employed to study the activitation and inhibition effects of APE1 in HeLa cells, respectively. As shown in Figure 5, the fluorescence signals in NCA-treated cells significantly decreased, whereas the fluorescence intensity in TBHP-treated cells obviously increased. Higher fluorescence signals could be observed with the increase of the amount of TBHP used to treat the cells. These results demonstrated that Nanoprobe A was capable of differentiate cells that express different levels of APE1 (7). The probe could also be used to screen stimulators and inhibitors of APE1 *in situ* in living cells.

Moreover, it has been reported that cancer cells usually have higher APE1 expression, suggesting that Nanoprobe A would be cleaved more efficiently inside cancer cells. This actually provides a new and very promising way to differentiate cancer cells from normal cells. Base on this unique property, Nanoprobe A may serve as a delivery tool for selective release of anti-cancer drugs in cancer cells. It also

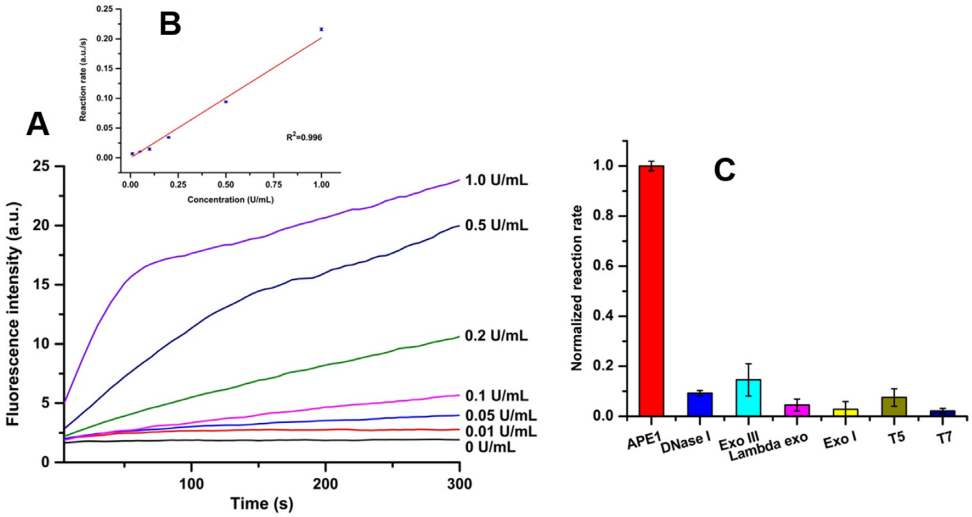

Figure 3. (**A**) Fluorescence responses of Nanoprobe A (0.1 mg/ml) to APE1 at different concentrations. (**B**) Linear calibration curve for detection of the activity of APE1. The linear regression equation is $F = 0.20\ c\ (\mathrm{U/ml}) - 2.1 \times 10^{-4}$, and the detection limit is 0.01 U/ml. (**C**) Selectivity of Nanoprobe A toward APE1 (2.0 U/ml) over other nucleases. (DNase I: 5.0 U/ml; Exo III: 4.0 U/ml; lambda exo: 66.7 U/ml; Exo I: 12.5 U/ml; T5: 5.0 U/ml; T7: 50 U/ml). All experiments were repeated at least three times.

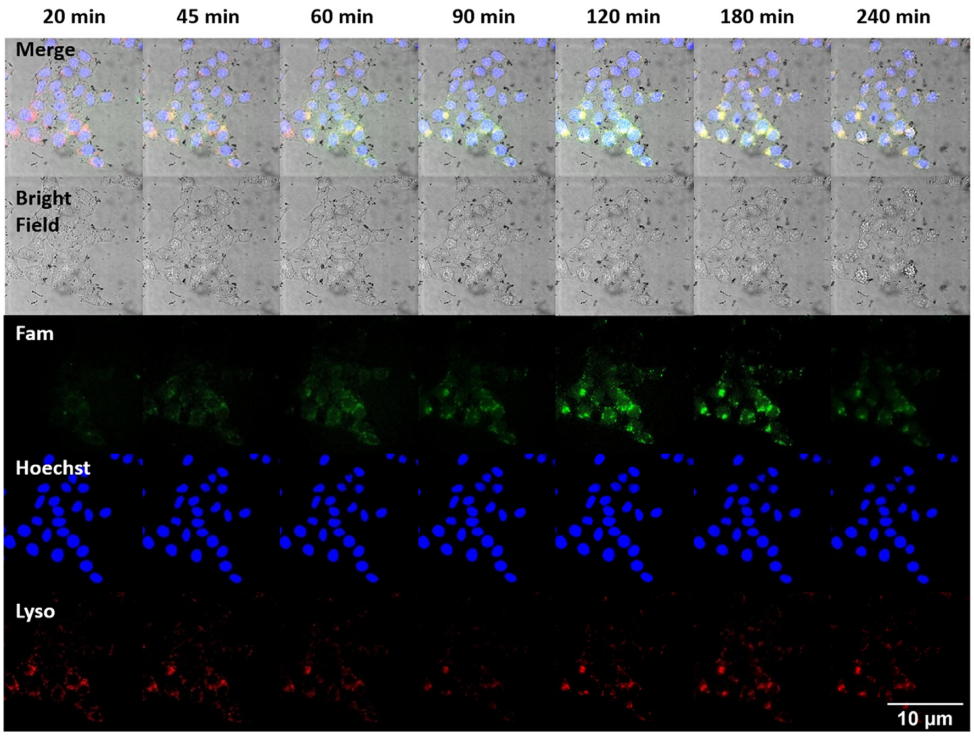

Figure 4. In-situ fluorescence imaging of the activity of APE1 in living cells by using Nanoprobe A. Cell nuclei and lysosome were stained with Hoechst 33342 (blue) and Lyso-Tracker Red, respectively.

holds great potential in exploring the roles of APE1 in regulating cellular responses and the mechanism.

CONCLUSIONS

In this work, we systematically investigated the effects of different conjugation strategies on the cleavage of DNA by several commonly existing nucleases in cells. For the first time, we report the specific interactions between APE1 and avidin. We demonstrated that biotin-labeled abasic site-containing dsDNA (AP-DNA) attached to the avidin-modified surface of SiMNPs can be specifically and efficiently cleaved by APE1 while resistant to the nonspecific digestion by other nucleases. The obtained Nanoprobe A could sensitively respond to APE1 at a concentration level as low as 0.01 U/ml. More importantly, the nanoprobe could be effectively internalized by living cells and enabled

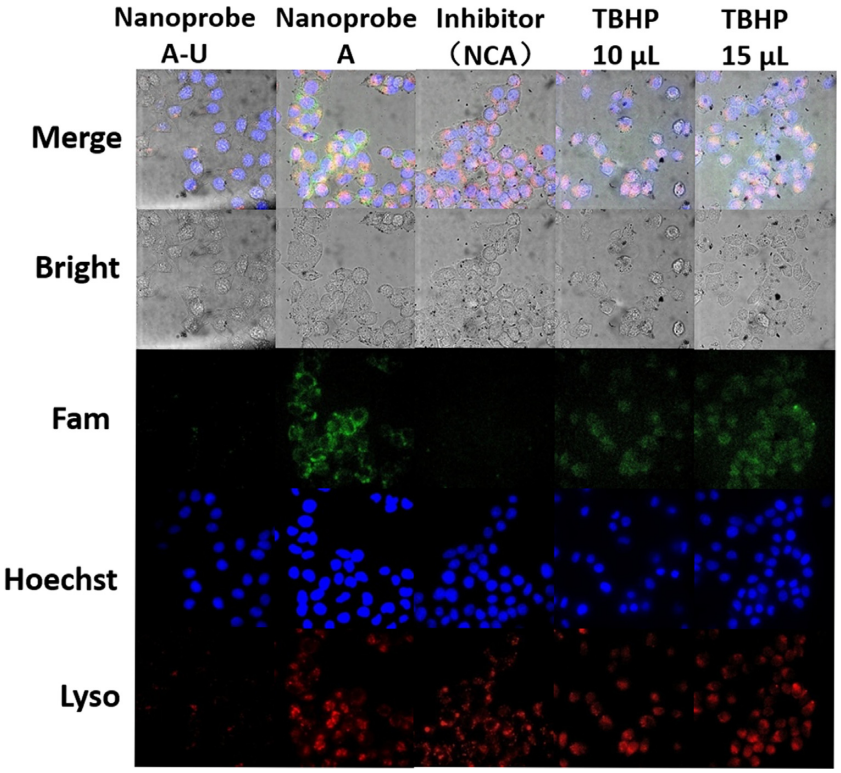

Figure 5. Confirmation of the cleavage of Nanoprobe A at the AP-site by APE1 in the intracellular environment. Nanoprobe A-U had the same sequence as Nanoprobe A except that the the uracil base was not removed by UDG treatment (see Supplementary Table S1).

cleavage of DNA sequence at the AP-site in the intracellular environment. This unique property offers the possibility of APE1-mediated cleavage of DNA sequence at predetermined site in the intracellular environment which are admired in intracellular imaging and cancer therapy since APE1 levels often increase in cancer cells. Furthermore, this nanoprobe realized for the first time in situ tracking of the variation of intracellular APE1 activity in response to different drugs. It holds great potential in exploring for the roles of APE1 in regulating cellular responses and also provides a useful tool for discovery of novel anti-cancer drugs.

SUPPLEMENTARY DATA

Supplementary Data are available at NAR Online.

FUNDING

National Natural Science Foundation of China [81571130100, 21575008 and 21375004]; Beijing Natural Science Foundation [2152014]. Funding for open access charge: National Natural Science Foundation of China.
Conflict of interest statement. None declared.

REFERENCES

1. Tell,G., Quadrifoglio,F., Tiribelli,C. and Kelley,M.R. (2009) The many functions of APE1/Ref-1: not only a DNA repair enzyme. *Antioxid. Redox Sign.*, **11**, 601–619.
2. Vascotto,C., Fantini,D., Romanello,M., Cesaratto,L., Deganuto,M., Leonardi,A., Radicella,J.P., Kelley,M.R., D'Ambrosio,C., Scaloni,A. *et al.* (2009) APE1/Ref-1 interacts with NPM1 within nucleoli and plays a role in the rRNA quality control process. *Mol. Cell. Biol.*, **29**, 1834–1854.
3. Evans,A.R., Limp-Foster,M. and Kelley,M.R. (2000) Going APE over ref-1. *Mutat. Res. DNA Repair*, **461**, 83–108.
4. Demple,B. and Sung,J.S. (2005) Molecular and biological roles of Ape1 protein in mammalian base excision repair. *DNA Repair (Amst.)*, **4**, 1442–1449.
5. Wilson,D.M. and Barsky,D. (2001) The major human abasic endonuclease: formation, consequences and repair of abasic lesions in DNA. *Mutat. Res. DNA Repair*, **485**, 283–307.
6. Tell,G., Damante,G., Caldwell,D. and Kelley,M.R. (2005) The intracellular localization of APE1/Ref-1: more than a passive phenomenon? *Antioxid. Redox Sign.*, **7**, 367–384.
7. Li,M. and Wilson,D.M. (2014) Human apurinic/apyrimidinic endonuclease 1. *Antioxid. Redox Sign.*, **20**, 678–707.
8. Robertson,K.A., Bullock,H.A., Xu,Y., Tritt,R., Zimmerman,E., Ulbright,T.M., Foster,R.S., Einhorn,L.H. and Kelley,M.R. (2001) Altered expression of Ape1/ref-1 in germ cell tumors and overexpression in NT2 cells confers resistance to bleomycin and radiation. *Cancer Res.*, **61**, 2220–2225.
9. Cesaratto,L., Codarin,E., Vascotto,C., Leonardi,A., Kelley,M.R., Tiribelli,C. and Tell,G. (2013) Specific inhibition of the redox activity of ape1/ref-1 by e3330 blocks tnf-alpha-induced activation of IL-8 production in liver cancer cell lines. *PLoS One*, **8**, e70909.
10. Han,J., Zhuo,Y., Chai,Y., Xiang,Y., Yuan,R., Yuan,Y. and Liao,N. (2013) Ultrasensitive electrochemical strategy for trace detection of APE-1 via triple signal amplification strategy. *Biosens. Bioelectron.*, **41**, 116–122.
11. Zhuo,Y., Liao,N., Chai,Y.Q., Gui,G.F., Zhao,M., Han,J., Xiang,Y. and Yuan,R. (2014) Ultrasensitive apurinic/apyrimidinic endonuclease 1 immunosensing based on self-enhanced electrochemiluminescence of a Ru(II) complex. *Anal. Chem.*, **86**, 1053–1060.
12. Leung,K.H., He,H.Z., Ma,V.P., Zhong,H.J., Chan,D.S., Zhou,J., Mergny,J.L., Leung,C.H. and Ma,D.L. (2013) Detection of base excision repair enzyme activity using a luminescent G-quadruplex selective switch-on probe. *Chem. Commun.*, **49**, 5630–5632.

13. Fang,S., Chen,L. and Zhao,M. (2015) Unimolecular chemically modified DNA fluorescent probe for one-step quantitative measurement of the activity of human apurinic/apyrimidinic endonuclease 1 in biological samples. *Anal. Chem.*, **87**, 11952–11956.
14. Qian,R.C., Ding,L. and Ju,H.X. (2013) Switchable fluorescent imaging of intracellular telomerase activity using telomerase-responsive mesoporous silica nanoparticle. *J. Am. Chem. Soc.*, **135**, 13282–13285.
15. Zhang,P., Cheng,F., Zhou,R., Cao,J., Li,J., Burda,C., Min,Q. and Zhu,J.J. (2014) DNA-hybrid-gated multifunctional mesoporous silica nanocarriers for dual-targeted and microRNA-responsive controlled drug delivery. *Angew. Chem. Int. Ed.*, **53**, 2371–2375.
16. Torney,F., Trewyn,B.G., Lin,V.S.-Y. and Wang,K. (2007) Mesoporous silica nanoparticles deliver DNA and chemicals into plants. *Nat. Nanotechnol.*, **2**, 295–300.
17. Liu,G., Swierczewska,M., Lee,S. and Chen,X. (2010) Functional nanoparticles for molecular imaging guided gene delivery. *Nano Today*, **5**, 524–539.
18. Mura,S., Nicolas,J. and Couvreur,P. (2013) Stimuli-responsive nanocarriers for drug delivery. *Nat. Mater.*, **12**, 991–1003.
19. Li,H.N., Mu,Y.W., Lu,J.S., Wei,W., Wan,Y.K. and Liu,S.Q. (2014) Target-cell-specific fluorescence silica nanoprobes for imaging and theranostics of cancer cells. *Anal. Chem.*, **86**, 3602–3609.
20. He,X.X., Wang,K.M., Tan,W.H., Liu,B., Lin,X., He,C.M., Li,D., Huang,S.S. and Li,J. (2003) Bioconjugated nanoparticles for DNA protection from cleavage. *J. Am. Chem. Soc.*, **125**, 7168–7169.
21. Roy,I., Ohulchanskyy,T.Y., Bharali,D.J., Pudavar,H.E., Mistretta,R.A., Kaur,N. and Prasad,P.N. (2005) Optical tracking of organically modified silica nanoparticles as DNA carriers: a nonviral, nanomedicine approach for gene delivery. *Proc. Natl. Acad. Sci. U.S.A.*, **102**, 279–284.
22. Bharali,D.J., Klejbor,I., Stachowiak,E.K., Dutta,P., Roy,I., Kaur,N., Bergey,E.J., Prasad,P.N. and Stachowiak,M.K. (2005) Organically modified silica nanoparticles: a nonviral vector for in vivo gene delivery and expression in the brain. *Proc. Natl. Acad. Sci. U.S.A.*, **102**, 11539–11544.
23. Ma,D., Guan,J., Normandin,F., Dénommée,S., Enright,G., Veres,T. and Simard,B. (2006) Multifunctional nano-architecture for biomedical applications. *Chem. Mater.*, **18**, 1920–1927.
24. Yu,C.J., Wu,S.M. and Tseng,W.L. (2013) Magnetite nanoparticle-induced fluorescence quenching of adenosine triphosphate-BODIPY conjugates: application to adenosine triphosphate and pyrophosphate sensing. *Anal. Chem.*, **85**, 8559–8565.
25. Cai,L., Chen,Z.Z., Chen,M.Y., Tang,H.W. and Pang,D.W. (2013) MUC-1 aptamer-conjugated dye-doped silica nanoparticles for MCF-7 cells detection. *Biomaterials*, **34**, 371–381.
26. Mol,C.D., Izumi,T., Mitra,S. and Tainer,J.A. (2000) DNA-bound structures and mutants reveal abasic DNA binding by APE1 and DNA repair coordination. *Nature*, **403**, 451–456.
27. Mitra,S., Izumi,T., Boldogh,I., Bhakat,K.K., Chattopadhyay,R. and Szczesny,B. (2007) Intracellular trafficking and regulation of mammalian AP-endonuclease 1 (APE1), an essential DNA repair protein. *DNA Repair*, **6**, 461–469.
28. Fishel,M.L. and Kelley,M.R. (2007) The DNA base excision repair protein Ape1/Ref-1 as a therapeutic and chemopreventive target. *Mol Aspects Med.*, **28**, 375–395.